We are IntechOpen, the world's leading publisher of Open Access books Built by scientists, for scientists

4,800
Open access books available

122,000
International authors and editors

135M
Downloads

Our authors are among the

154
Countries delivered to

TOP 1%
most cited scientists

12.2%
Contributors from top 500 universities

CLARIVATE ANALYTICS BOOK CITATION INDEX INDEXED

WEB OF SCIENCE™

Selection of our books indexed in the Book Citation Index in Web of Science™ Core Collection (BKCI)

Interested in publishing with us?
Contact book.department@intechopen.com

Numbers displayed above are based on latest data collected.
For more information visit www.intechopen.com

1

Concentration-Dependent Laser Performance of Yb:YAG Ceramics and Passively Q-switched Yb:YAG/Cr,Ca:YAG Lasers

Jun Dong[1], Ken-ichi Ueda[2], Hideki Yagi[3] and Alexander A Kaminskii[4]
[1]*Department of Electronic Engineering, Xiamen University*
[2]*Institute for Laser Science, University of Electro-Communications*
[3]*Konoshima Chemical Co. Ltd.*
[4]*Institute of Crystallography, Russian Academy of Science*
[1]*P. R. China*
[2,3]*Japan*
[4]*Russia*

1. Introduction

Ytterbium doped laser materials have been intensely investigated for developing high power laser-diode pumped solid-state lasers around 1 μm (Krupke 2000). Yb:YAG as crystals and polycrystalline ceramics are one of the dominant laser gain media used for solid-state lasers (Lacovara et al., 1991; Brauch et al., 1995; Bruesselbach et al., 1997; Taira et al., 1997; Dong et al., 2006) owing to the excellent optical, thermal, chemical and mechanical properties (Bogomolova et al., 1976). Owing to the small radius difference between yttrium ions and ytterbium ions (Dobrzycki et al., 2004), Yb:YAG single-crystal doped with different Yb concentrations can be grown by different crystal growth methods and efficient laser performance has been achieved (Brauch et al., 1995; Patel et al., 2001; Dong et al., 2006). Transparent laser ceramics (Lu et al., 2000; Lu et al., 2001; Lu et al., 2002; Takaichi et al., 2003; Dong et al., 2006) fabricated by the vacuum sintering technique and nanocrystalline technology (Yanagitani et al., 1998) have been proven to be potential replacements for counterpart single crystals because they have several remarkable advantages compared with single-crystal laser materials, such as high concentration and easy fabrication of large-size ceramics samples, multilayer and multifunctional ceramics laser materials (Yagi et al., 2006; Dong et al., 2007). Efficient and high power laser operation in Nd^{3+}- and Yb^{3+}-ions doped YAG ceramics has been demonstrated (Lu et al., 2002; Dong et al., 2006). Yb:YAG has been a promising candidate for high-power laser-diode pumped solid-state lasers with rod (Honea et al., 2000), slab (Rutherford et al., 2000), and thin disk (Giesen et al., 1994; Stewen et al., 2000) configurations. The quasi-three-level laser system of Yb:YAG requires high pumping intensity to overcome transparency threshold and achieve efficient laser operation at room temperature (Dong & Ueda 2005). The thin disk laser has been demonstrated to be a good way to generate high power with good beam quality owing to the efficiently cooling of gain medium and good overlap of the pump beam and laser beam (Giesen et al., 1994). However, in the thin disk case, the pump beam must be folded many times into thin laser gain

Source: Advances in Solid-State Lasers: Development and Applications, Book edited by: Mikhail Grishin,
ISBN 978-953-7619-80-0, pp. 630, February 2010, INTECH, Croatia, downloaded from SCIYO.COM

medium disk with mirrors in order to absorb sufficient pump power, which makes the laser system extremely complicated. Some applications require that the lasers should be compact and economic; therefore, the cooling system is eliminated in compact and easily maintainable laser system. Therefore, laser-diode end-pumped microchip lasers are a better choice to achieve highly efficient laser operation under high pump power intensity. The thinner the gain medium, the better the cooling effect, therefore, heavy doped Yb:YAG gain media are the better choice for such lasers. The development of Yb:YAG ceramics doped with 1 at.% Yb^{3+} ions have been reported (Takaichi et al., 2003), but the efficiency of such Yb:YAG ceramic laser is low owing to the deficient activator concentration. In principle, there is no concentration quenching effect in Yb:YAG, however, the unwanted impurities (such as Er^{3+}, Tm^{3+}, Ho^{3+}, and so on) from raw materials will be deleterious to the laser performance owing to the high activator doping. Concentration dependent optical properties and laser performance of Yb:YAG crystals have been reported(Yin et al., 1998; Qiu et al., 2002; Yang et al., 2002; Dong et al., 2007). The concentration quenching of Yb:YAG crystals has been investigated and it was found that fluorescence lifetime decreases when the Yb concentration is greater than 15 at.% and lifetime decreases up to 15% when the Yb concentration reaches to 25 at.% (Sumida & Fan 1994; Yang et al., 2002). The fluorescence lifetime of Yb^{3+} doped materials is usually affected by the radiative trapping and concentration quenching effects (M. Ito et al., 2004). Radiative trapping and concentration quenching effects become stronger with Yb concentration and there is a concentration region (from 15 to 25 at.% for Yb:YAG crystal), two trends compete each other and consequently compensate each other, leading to a constant value of measured fluorescence lifetime. Therefore special technologies have been taken to eliminate the radiative trapping effect when the fluorescence lifetime is measured for Yb doped materials. Optical-thin samples or powder sandwiched between two undoped YAG crystals were used to measure the radiative lifetime of Yb:YAG crystals (Sumida & Fan 1994; Patel et al., 2001). The radiative lifetime of Yb:YAG crystal was found to decrease with Yb concentration. Optical spectra of Yb:YAG ceramics doped with different Yb^{3+}-lasant concentration (C_{Yb} = 9.8, 12, and 20 at.%) and efficient 9.8 at.% Yb:YAG ceramic microchip lasers (Dong et al., 2006) have been reported recently. The comparison of laser performance of Yb:YAG ceramic and single-crystal doped with 20 at.% Yb has been reported (Dong et al., 2007). However, there is no systematic comparison studies of microchip laser performance of Yb:YAG ceramics and single-crystal doped with different Yb concentrations.

Compact, high beam quality laser-diode pumped passively Q-switched solid-state lasers with high peak power are potentially used in optical communications, pollution monitoring, nonlinear optics, material processing and medical surgery, and so on(Zayhowski 2000). Passively Q-switched solid-state lasers are usually achieved by using neodymium or ytterbium doped crystals as gain media and Cr,Ca:YAG as saturable absorber(Zayhowski & Dill III 1994; Lagatsky et al., 2000; Takaichi et al., 2002; Dong et al., 2006) or semiconductor saturable absorber mirror (SESAM)(Spuhler et al., 2001) as saturable absorber. Compared with SESAM, Cr^{4+} doped bulk crystals as saturable absorber have several advantages, such as high damage threshold, low cost, and simplicity. The output pulse energy from passively Q-switched solid-state lasers is inversely proportional to the emission cross section of gain medium and reflectivity of the output coupler according to the passively Q-switched theory(Degnan 1995). Besides the broad absorption spectrum (Bruesselbach et al., 1997), longer fluorescence lifetime(Sumida & Fan 1994), high quantum efficiency (over 91% with

pump wavelength of 941 nm and laser wavelength of 1030 nm) (Fan 1993) of Yb:YAG gain medium and easy growth of high quality and moderate concentration crystal without concentration quenching (Patel et al., 2001), smaller emission cross section of Yb:YAG (about one tenth of that for Nd:YAG) (Dong et al., 2003) is more suitable to obtain high pulse energy output than Nd:YAG in passively Q-switched solid-state lasers. Another interest in Yb:YAG lasers is that the frequency doubled wavelength of 515 nm matches the highest power line of Ar-ion lasers, thereby leading to the possibility of an all solid-state replacement (Fan & Ochoa 1995). Linearly polarized laser output was observed in these compact passively Q-switched lasers (Li et al., 1993; Yankov 1994; Kir'yanov et al., 1999; Yoshino & Kobyashi 1999; Dong et al., 2000; Bouwmans et al., 2001). The causes of the linearly polarized output in these passively Q-switched lasers were attributed to the influence of the pump polarization(Bouwmans et al., 2001), relative orientations of the switch and an intracavity polarizer(Kir'yanov et al., 1999), temperature change induced weak phase anisotropy(Yoshino & Kobyashi 1999), and the anisotropic nonlinear saturation absorption of Cr,Ca:YAG crystal under high laser intensity(Eilers et al., 1992). The anisotropic nonlinear absorption of Cr,Ca:YAG crystal induced linearly polarization in passively Q-switched lasers with Cr,Ca:YAG as saturable absorber held until appearing of transparent rare-earths doped YAG laser ceramics(Lu et al., 2002; Dong et al., 2006). Efficient laser operation in Nd^{3+}:YAG and Yb^{3+}:YAG ceramic lasers has been demonstrated(Lu et al., 2002; Dong et al., 2006; Nakamura et al., 2008). Chromium doped YAG ceramic has also been demonstrated to be a saturable absorber for passively Q-switched Nd:YAG and Yb:YAG ceramic lasers(Takaichi et al., 2002; Dong et al., 2006). Recently, laser-diode pumped passively Q-switched Yb:YAG/Cr:YAG all-ceramic microchip laser has been demonstrated(Dong et al., 2006), and pulse energy of 31 μJ and pulse width of 380 ps have been achieved with 89% initial transmission of the Cr,Ca:YAG ceramic as saturable absorber and 20% transmission of the output coupler. However, there is coating damage occurrence because of the high energy fluence with low transmission of the output coupler. There are two ways to solve the coating damage problem: one is to improve the coating quality on the gain medium which is costly; the other is to increase the transmission of the output coupler to decrease the intracavity pulse energy fluence. Therefore, 50% transmission of the output coupler was used to balance the output pulse energy and intracavity pulse energy, for this case, the initial transmission of Cr,Ca:YAG can be further decreased to obtain high energy output according to the passively Q-switched solid-state laser theory(Degnan 1995). The laser performance of passively Q-switched Yb:YAG/Cr,Ca:YAG all-ceramic microchip laser was further improved by using 20% initial transmission of the Cr,Ca:YAG ceramic as saturable absorber and 50% transmission of the output coupler, and no coating damage were observed with high pump power(Dong et al., 2007). Highly efficient, sub-nanosecond pulse width and high peak power laser operation has been observed in Yb:YAG/Cr^{4+}:YAG composite ceramics(Dong et al., 2007; Dong et al., 2007). Although linearly polarized states was reported in passively Q-switched Nd:YAG/Cr,Ca:YAG ceramic lasers(Feng et al., 2004), the extinction ratio was very small. The crystalline-orientation self-selected linearly polarized, continuous-wave operated microchip lasers were demonstrated by adopting [111]-cut Yb:YAG crystal(Dong et al., 2008) and [100]-cut Nd:YAG crystal(McKay et al., 2007) as gain medium.

Here, we report on the systematical comparison of the performance of miniature Yb:YAG (C_{Yb} = 9.8, 12, and 20 at.%) ceramic and Yb:YAG single-crystals (C_{Yb} = 10, 15, and 20 at.%)

lasers at 1030 nm with two-pass pumping scheme. The laser performance of Yb:YAG ceramics is nearly comparable to or better than their counterpart single crystals depending on the Yb doping concentration. The effect of Yb concentration on the optical-to-optical efficiency and laser emitting spectra was also addressed. The polarization states of passively Q-switched Yb:YAG/Cr,Ca:YAG microchip lasers with Yb:YAG crystal or ceramic as gain medium and Cr,Ca:YAG crystal or ceramic as saturable absorber were also presented. Based on our previous experiments and results of passively Q-switched Yb:YAG/Cr,Ca:YAG microchip lasers, 20% initial transmission of the saturable absorber and 50% transmission of the output coupler were used in the experiments to compare the polarization states and the effect of the polarization states on the laser performance of these passively Q-switched microchip laser. Linearly polarized states were observed in Yb:YAG/Cr,Ca:YAG combinations with at least one crystal. For Yb:YAG/Cr,Ca:YAG all-ceramics combination, the laser oscillates at random polarization state. The effect of polarized states of passively Q-switched Yb:YAG/Cr,Ca:YAG lasers on the laser performance was also investigated.

2. Experiments

To compare the laser performance of Yb:YAG ceramics and single-crystals, double-pass pumped miniature lasers were used in the experiments. To absorb sufficient pump power, high doping concentration was needed for thin gain medium. Therefore, high doping concentration Yb:YAG single-crystals and ceramics were used in the laser experiments. Three Yb:YAG ceramics samples (C_{Yb} = 9.8, 12, and 20 at.%) were used in the laser experiments. Comparable Yb:YAG single-crystals (C_{Yb} = 10, 15, and 20 at.%) were used to compare the laser characteristics with those of Yb:YAG ceramics. The size of the samples is 10 mm in diameter and 1 mm in thickness. The absorption spectra of Yb:YAG crystals and ceramics were measured by using a ANDO white light source and an optical spectral analyzer (ANDO AQ6137). Emission spectra were measured at 900 – 1150 nm with a fiber-coupled diode laser operating at 940 nm as the pump source. The pump light was focused into one of the ground surfaces of the sample close to the polished surface through which the emitted fluorescence was to be observed. As a result the fluorescent light detected was generated close to the surface from which it exited the sample, such that it experienced minimal radiation trapping. The fluorescence emission spectral signal was collected by using a focus lens and coupled into a multi-mode fiber which was connected to an optical spectral analyzer. The resolution of the optical spectral analyzer is 0.01 nm. The effective emission cross section of Yb:YAG crystals and ceramics was calculated by applying Fuechtbauer-Ladenburg formula. The absorption and emission spectra of Yb:YAG ceramics and single-crystals doped with different ytterbium concentrations were measured at room temperature. Fig. 1 shows the room temperature absorption and emission spectra of Yb:YAG ceramic and single-crystal containing 20 at.% of ytterbium activators. The absorption and emission spectra of Yb:YAG ceramics are nearly identical to those of Yb:YAG single crystals. However there were some differences between Yb:YAG crystals and ceramics which may have potential effects on the laser performance. Firstly, the absorption coefficient of Yb:YAG ceramics is higher than that of Yb:YAG single crystal for the same Yb doping concentration. The peak absorption coefficient at 940 nm increases linearly with Yb activator concentration for both Yb:YAG ceramics and single-crystals, as shown in the inset of Fig. 1(a), the peak absorption coefficients at 940 nm of low doping concentraiton Yb:YAG samples were taken from Ref. (Dong et al., 2003; Takaichi et al., 2003). However, the

absorption coefficient of Yb:YAG single-crystals increases slowly with Yb concentration compared to Yb:YAG ceramics. And the absorption coefficient of Yb:YAG ceramics is about 10% more than that for the counterpart single-crystal with same doping levels at high doping levels. This was caused by the segregation in Yb:YAG single crystal during the crystal growth and the Yb^{3+} concentration is lower than that in melt. This effect becomes more obvious at high doping levels. However, Yb^{3+} ions are uniformly distributed in the mixed Yb:YAG nanocrystalline power. Secondly, there were some differences between the emission cross section of Yb:YAG ceramics and crystals. Fig. 1(b) shows the emission spectra of Yb:YAG ceramic and single-crystals doped with 20 at.% Yb^{3+}-ions. Two main emission peaks are centered at 1030 nm and 1049 nm. The effective peak emission cross section of Yb:YAG ceramics was estimated to be 2.2×10^{-20} cm^2 at 1030 nm, which was lower than that of Yb:YAG single-crystal (2.3×10^{-20} cm^2). The effective emission cross section at 1047.5 nm (0.37×10^{-20} cm^2) was about one sixth of that at 1030 nm for Yb:YAG ceramics. However, the effective emission cross section at 1046.9 nm (0.39×10^{-20} cm^2) of Yb:YAG crystal is 5% higher than that of Yb:YAG ceramics. The lower effective emission cross section of Yb:YAG ceramics limits the laser performance under the same laser conditions as that for Yb:YAG crystals. The emission cross section of Yb:YAG ceramics does not change with Yb concentration, which is in good agreement with the measured emission cross section of Yb:YAG single-crystals (Dong et al., 2003) although the emission intensity increases with increase of the Yb concentrations.

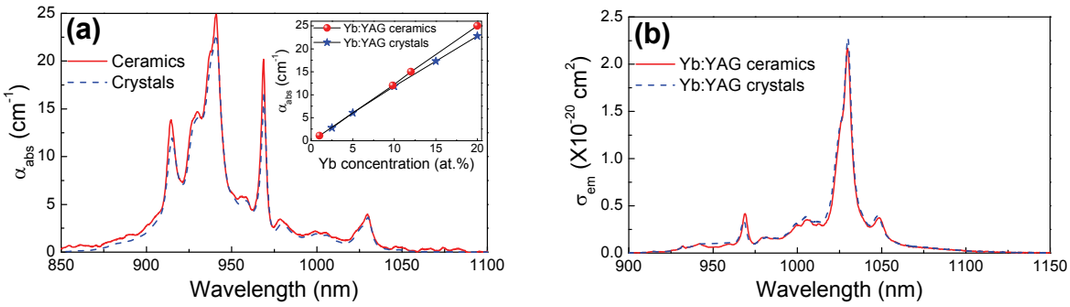

Fig. 1. The absorption and emission spectra of Yb:YAG ceramic and single-crystal doped with 20 at.% Yb at room temperature. Inset in Fig.1(a) shows the 940-nm peak absorption coefficient of Yb:YAG ceramics and single-crystals as a function of Yb concentrations.

Fig. 2 shows a schematic diagram of the experimental setup for laser-diode pumped Yb:YAG miniature laser. One surface of the sample was coated for antireflection both at 940 nm and 1.03 μm. The other surface was coated for total reflection at both 940 nm and 1.03 μm, acting as one cavity mirror and reflecting the pump power for increasing the absorption of the pump power. Plane-parallel fused silica output couplers with transmission (T_{oc}) of 5 and 10% were mechanically attached to the gain medium tightly. A 35-W high-power fiber-coupled 940 nm laser diode (Apollo, F35-940-1) with a core diameter of 100 μm and numerical aperture of 0.22 was used as the pump source. Optical coupling system with two lenses M1 (8-mm focal length) and M2 (15-mm focal length) was used to focus the pump beam on the ceramic rear surface and to produce a pump light footprint on the Yb:YAG of about 170 μm in diameter. The laser spectrum was analyzed by using an optical spectrum analyzer (ANDO AQ6137) with resolution of 0.01 nm. Output beam profile of these lasers

was monitored by using a CCD camera, and beam quality factor, M^2, was determined by measuring the beam diameters at different positions along the laser propagation direction.

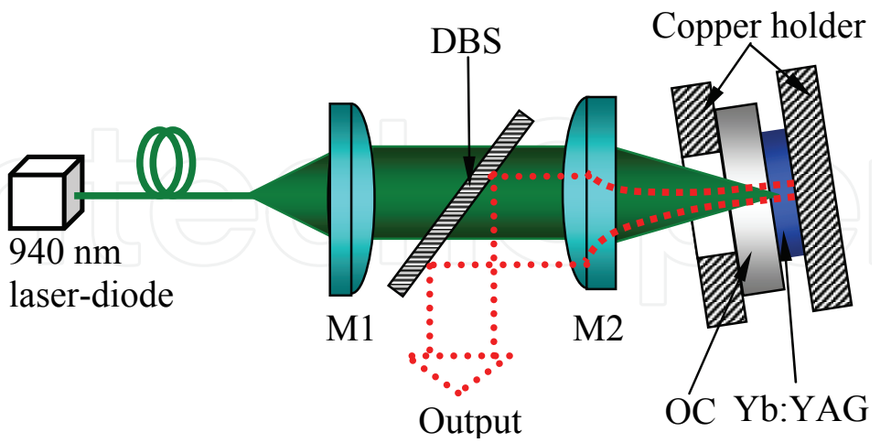

Fig. 2. Schematic diagram of laser-diode pumped Yb:YAG ceramics and single-crystals miniature lasers. DBS, dichroic beam splitter; OC, output coupler; M1, focus lenses with focal length of 8 mm; M2, focus lenses with focal length of 15 mm.

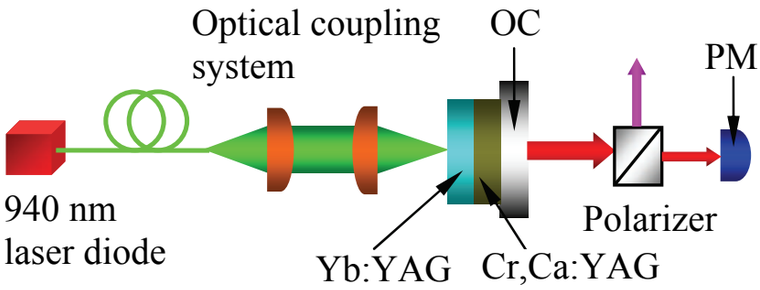

Fig. 3. Schematic diagram for passively Q-switched Yb:YAG microchip lasers with Cr,Ca:YAG as saturable absorber. OC, output coupler; PM, power meter.

Fig. 3 shows a schematic diagram of experimental setup for passively Q-switched Yb:YAG microchip laser with Cr,Ca:YAG as saturable absorber. Two Yb:YAG samples are used as gain media, one is Yb:YAG ceramic doped with 9.8 at.% Yb, the other is [111]-cut Yb:YAG crystal doped with 10 at.% Yb. The thickness of Yb:YAG samples is 1 mm, and the Yb:YAG samples are polished to plane-parallel. One surface of the gain medium was coated for anti-reflection at 940 nm and total reflection at 1.03 μm acting as one cavity mirror. The other surface was coated for high transmission at 1.03 μm. Two 1-mm-thick, uncoated Cr,Ca:YAG ceramic and [111]-cut Cr,Ca:YAG crystal with 80% initial transmission, acting as Q-switch, was sandwiched between Yb:YAG sample and a 1.5-mm-thick, plane-parallel fused silica output coupler with 50% transmission. Total cavity length was 2 mm. The initial charge concentration of $CaCO_3$ and Cr_2O_3 in growth of Cr,Ca:YAG crystal and fabrication of Cr,Ca:YAG ceramic are 0.2 at.% and 0.1 at.%, respectively. The absorption center of Cr,Ca:YAG sample centered at 1 μm is also strongly affected by the annealing process and the exact concentration of this absorption center is difficult to determine, the concentration center of this absorption is roughly about 4% of the initial Cr doping concentration

(Okhrimchuk & Shestakov 1994). Therefore, the initial transmission of the Cr,Ca:YAG saturable absorber is usually used in comparing the laser performance of passively Q-switched lasers. The initial transmission of Cr,Ca:YAG is governed by the doping concentration and the thickness of the sample, to fully compare laser performance with our previously passively Q-switched Yb:YAG/Cr,Ca:YAG all-ceramic microchip laser and the effect of polarization states on the passively Q-switched Yb:YAG/Cr,Ca:YAG microchip lasers, 1-mm-thick Cr,Ca:YAG crystal with 80% initial transmission was used in the experiment. It should be noted that the polarization behavior keeps the same if a different modulation depth of Cr,Ca:YAG saturable absorber is used. A high-power fiber-coupled 940 nm laser diode with a core diameter of 100 μm and numerical aperture of 0.22 was used as the pump source. Two lenses of 8-mm focal length were used to focus the pump beam on the Yb:YAG rear surface and to produce a pump light footprint on the Yb:YAG of about 100 μm in diameter. The laser was operated at room temperature. The Q-switched pulse profiles were recorded by using a fiber-coupled InGaAs photodiode with a bandwidth of 16 GHz, and a 7 GHz Tektronix TDS7704B digital phosphor oscilloscope. The laser spectrum was analyzed by using an optical spectrum analyzer. The laser output beam profile was monitored using a CCD camera both in the near-field and the far-field of the output coupler.

3. Results and discussion

3.1 Continuous-wave Yb:YAG miniature lasers

Fig. 4 shows the output power of miniature Yb:YAG ceramics and single-crystal lasers as a function of the absorbed pump power for different Yb concentrations and T_{oc}. The absorbed pump power for reaching laser thresholds of Yb:YAG ceramics (C_{Yb} = 9.8, 12, and 20 at.%) were 0.3, 0.33, and 0.64 W for T_{oc} = 5% and 0.33, 0.5, 0.68 W for T_{oc} = 10%. The pump power threshold increases with T_{oc} and Yb concentration for Yb:YAG ceramic lasers. This was caused by the increase of the losses introduced by the large T_{oc} and the increasing reabsorption of Yb^{3+} at lasing wavelength with Yb concentrations. For Yb:YAG ceramics doped with different Yb concentrations, the output power increases linearly with absorbed pump power for T_{oc} = 5 and 10%. The slope efficiencies respected to the absorbed pump power for Yb:YAG ceramics (C_{Yb} = 9.8, 12, and 20 at.%) were measured to be 50, 55, and 45% for T_{oc} = 5% and 52, 44, and 38% for T_{oc} = 10%. Slope efficiency increases with T_{oc} for 9.8 at.% Yb:YAG ceramic, however, the slope efficiencies decrease with T_{oc} for Yb:YAG ceramics doped with 12 and 20 at.% Yb^{3+} ions. Maximum output power of 2.54 W was measured for T_{oc} = 5% by using 12 at.% Yb:YAG ceramic as gain medium when the absorbed pump power was 5.3 W. The corresponding optical-to-optical efficiency was about 48%.

The absorbed pump power for reaching laser thresholds of Yb:YAG single-crystal (C_{Yb} = 10, 15, and 20 at.%) were 0.3, 0.51 and 0.76 W for T_{oc} = 5% and 0.35, 0.55, and 0.84 W for T_{oc} = 10%. The absorbed pump power threshold increases with the T_{oc} and Yb concentrations, the same tendency as that for Yb:YAG ceramics. However, the absorbed pump power thresholds of Yb:YAG single crystals were higher than those of Yb:YAG ceramics. This may be caused by the pump configuration used in the laser experiments and low pump power intensity with pump beam diameter of 170 μm. Because the incident pump beam from laser-diode is several degrees away from the normal direction of the laser beam, there is a mismatch between the pump beam and laser beam. From Fig. 4 (b), we can see at low pump power just above absorbed pump power threshold, the laser performance is lower than that

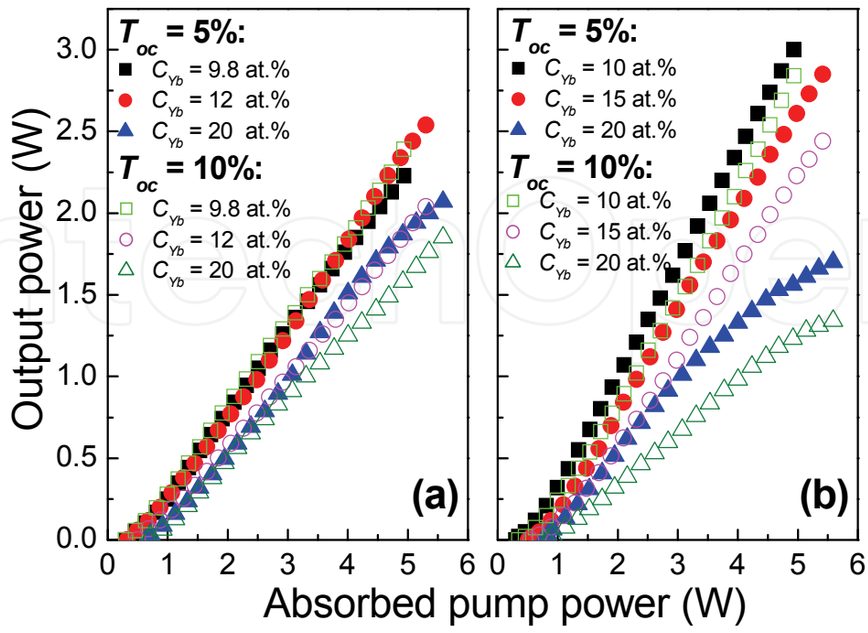

Fig. 4. Output power of (a) Yb:YAG ceramic and (b) Yb:YAG single crystal miniature lasers as a function of absorbed pump power for different Yb concentrations and transmissions of the output couplings.

high pump power levels, this is normal for the quasi-three-level system; efficient laser performance can be achieved at high pump power density (Dong & Ueda 2005). However, for Yb:YAG ceramics, owing to the random distribution of Yb:YAG crystalline particles, the absorbed pump power threshold can be achieved more easily. Output power increases linearly with absorbed pump power for Yb:YAG single-crystals doped with 10 and 15 at.% Yb. The slope efficiencies of miniature lasers based on Yb:YAG single-crystals doped with 10 and 15 at.% Yb were measured to be 69, 62% for T_{oc} = 5% and 67, 55% for T_{oc} = 10%. The slope efficiencies of Yb:YAG crystals doped with 10 and 15 at.% Yb^{3+} were higher than those for Yb:YAG ceramics although the pump power thresholds were higher than those of Yb;YAG ceramics. At higher pump power density, the inversion population excited by the pump beam is well-over the threshold, and the modes matched very well, therefore, the laser oscillates at high slope efficiency, especially for Yb:YAG crystal doped with 10 and 15 at.% Yb. The better laser performance of these crystals compared to their counterpart ceramic suggests that the intacavity loss for Yb:YAG crystal lower than that of Yb:YAG ceramics.

For Yb:YAG single-crystal doped with 20 at.% Yb, the output power increases with the absorbed pump power, and tends to increase slowly when the absorbed pump power is higher than a certain value (e.g. 3 W for T_{oc} = 5% and 2.3 W for T_{oc} = 10%), as shown in Fig. 4(b). However, besides the higher absorbed pump power threshold compared to its counterpart Yb:YAG ceramic, the slope efficiencies (45% for T_{oc} = 5% and 32 at.% for T_{oc} = 10%) of 20 at.% Yb:YAG single crystal were lower than those (47% for T_{oc} = 5% and 38 at.% for T_{oc} = 10%) for its counterpart Yb:YAG ceramic. The laser results show that heavy doped

Yb:YAG ceramic is better than its single crystal counterpart. The strong segregation of the impurities in Yb:YAG crystal with increase of the Yb concentration during crystal growth is the main reason for the worse laser performance. The other reasons for the less efficient laser operation may be the impurities increases with doping concentration (Yin et al., 1998), the impurities induced concentration quenching effect limit the laser performance of highly doped Yb:YAG crystals. The green emission was observed in the Yb:YAG crystals and ceramics when they were pumped with laser-diodes, and visible intensity increases with Yb concentration up to 15 at.% and then decreases with Yb concentration (Xu et al., 2005). Energy transfer from Yb^{3+} ions to Er^{3+} and Tm^{3+} impurities and cooperative energy transfer between Yb^{3+} ions are the causes of these visible luminescence. These are deleterious to the infrared laser operation. However, the distance between Yb^{3+} ions and impurities or other quenching centers is decreased with Yb concentration, the cooperative luminescence intensity decreases because the excited ions are more easily quenched by reaching a neighboring defect site. Therefore, the effect of cooperative energy transfer is not a main factor to limit the laser performance of highly doped Yb:YAG crystals.

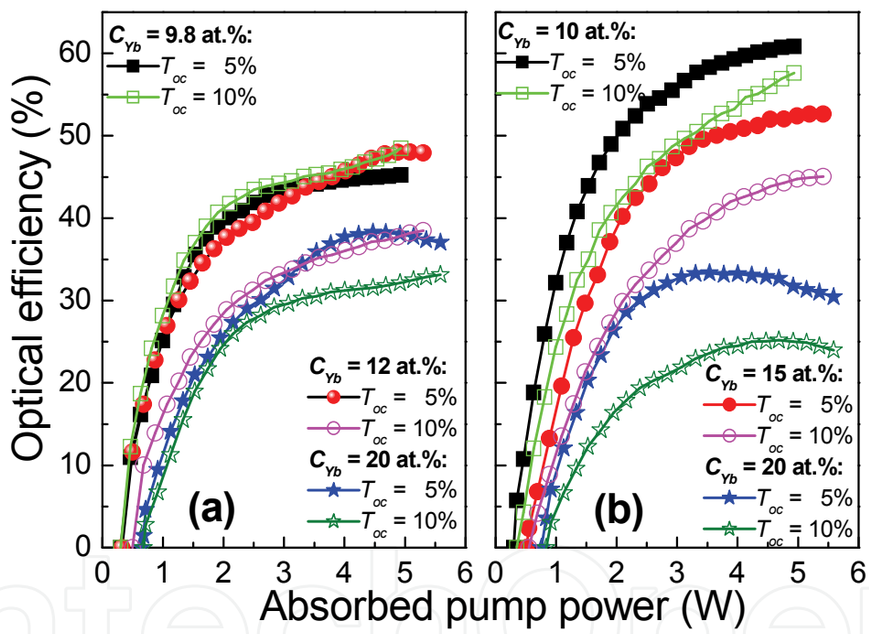

Fig. 5. Optical efficiencies of (a) Yb:YAG ceramic and (b) Yb:YAG single crystal miniature laser as a function of absorbed pump power for different Yb concentrations and transmissions of the output coupler.

Fig. 5 shows the optical-to-optical efficiencies of Yb:YAG lasers as a function of absorbed pump power. Under present laser experimental conditions, there is no saturation effect of Yb:YAG lasers with different output couplings for Yb concentration equal to or less than 15 at.% although the optical efficiency increases slowly with the absorbed pump power. However, for 20 at.% Yb:YAG, there is saturation effect for ceramic lasers with T_{oc} = 5% and for single-crystal lasers with different output couplings. Maximum optical efficiency of 48% was achieved for Yb:YAG ceramic doped with 12 at.% Yb at the absorbed pump power of

5.3 W. For single crystal doped with 20 at.% Yb lasants, there is a maximum optical efficiency for all output couplings [as shown in Fig. 5(b)]. The optical-to-optical efficiency decreases with further increase of the pump power. For Yb:YAG ceramics, except the comparable laser performance of 9.8 at.% Yb:YAG with T_{oc} = 5 and 10%, the optical-to-optical efficiency decreases with T_{oc} and Yb concentration. However, for Yb:YAG single-crystals, the optical-to-optical efficiency decreases with the T_{oc} and Yb concentration under different pump power levels. Optical-to-optical efficiency of Yb:YAG crystal doped with less than 15 at.% Yb is higher than that for Yb:YAG ceramics under certain pump power levels. For 20 at.% Yb:YAG, Yb:YAG ceramic has higher optical-to-optical efficiency than that of crystal under different pump power levels. The decrease of the optical-to-optical efficiency of Yb:YAG lasers with Yb concentration was attributed to the thick samples used for highly doped Yb:YAG samples. The better laser performance can be further improved through optimizing the thicknesses for Yb:YAG samples with different Yb concentrations. The highly efficient microchip lasers has been demonstrated by using the same crystals (Dong et al., 2007) as those here used.

Fig. 6 shows the maximum optical-to-optical efficiency under available pump power of Yb:YAG ceramics and single-crystals lasers as a function of Yb concentrations for different output couplings. For Yb:YAG single crystals, the maximum optical-to-optical efficiency decreases with Yb concentrations, there are 45% and 56% dropping for T_{oc} = 5 and 10% when Yb concentration increases from 10 at.% to 20 at.%. However, for Yb:YAG ceramics, the maximum optical-to-optical efficiency decreases with Yb concentration, the decrease is smaller for Yb:YAG ceramics compared to that for Yb:YAG single crystal. There are 15 and 32% dropping for T_{oc} = 5 and 10% when Yb concentration increases from 9.8 to 20 at.% for Yb:YAG ceramics. Because small different optical properties were observed in Yb:YAG ceramics and single-crystals doped with different Yb concentrations(Dong et al., 2003; Dong et al., 2006), the different laser performance of Yb:YAG ceramics and single-crystals may be caused by the Yb^{3+}-ions distribution in YAG host and optical quality of Yb:YAG samples. Although the distribution coefficient of Yb in Yb:YAG is close to unit, there is still concentration gradient observed in Yb:YAG single crystals along the growth axis and radius of the crystal boule (Xu et al., 2003). The Yb^{3+}-ion distribution inhomogeneity in Yb:YAG single-crystal becomes server with Yb concentration. The impurities such as Ho^{3+}, Er^{3+} increase with Yb concentration in Yb:YAG crystals because the strong segregation of rare-earth ions in YAG crystal was observed. This was observed in the reduced radiative lifetime in highly doped Yb:YAG crystals (Sumida & Fan 1994; Yin et al., 1998; Patel et al., 2001). This concentration quenching effect limits the efficient laser performance of highly doped Yb:YAG crystals. For ceramics, the distribution of Yb ions in the grains and grain boundary is a main factor to determine the optical properties. The gain boundary of YAG ceramics was measured to be less than 0.5 nm (Barabanenkov et al., 2004), and sintering temperature is about 200 ^{o}C lower than the melt point of Yb:YAG crystal, the segregation of Yb in grain boundary can only be achieved by diffusion or migration, therefore the distribution of Yb in gain and boundary should be close to homogeneous. When Yb ions were doped in YAG ceramics, the segregation of ytterbium ions in the grain boundary, accompanied by a reduction of the acoustic mismatch, leads to increased phonon transmission (Bisson et al., 2007). This will be further enhanced by introducing more ytterbium ions. This may be one of the main reasons for the better laser performance of heavy doped Yb:YAG ceramics compared to that of single-crystal with same doping levels.

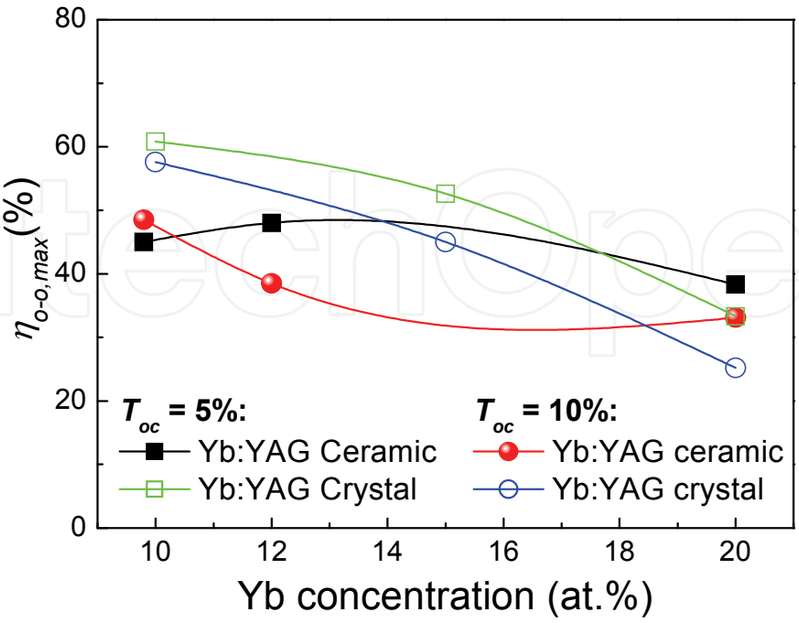

Fig. 6. Comparison of the maximum optical-to-optical efficiency of Yb:YAG miniature lasers as a function of Yb concentration. The solid lines were used for illustration.

Fig. 7 shows the comparison of the laser emitting spectra of 9.8 at.% Yb:YAG ceramic and 10 at.% Yb:YAG single-crystal miniature lasers under different absorbed pump power for T_{oc} = 5, and 10%. Lasers operated at multi-longitudinal modes under different pump levels. The number of longitudinal modes increases with the absorbed pump power because the inversion population provided with pump power can overcome the threshold for low gain away from the highest emission peak of Yb:YAG gain medium. The longitudinal mode oscillation for these miniature Yb:YAG lasers was mainly caused by the etalon effect of plane-parallel Yb:YAG thin plate. The separation of longitudinal modes was measured to be 0.29 nm, which is in good agreement with the free spectral range (0.292 nm) of 1-mm-long cavity filled with gain medium predicted by (Koechner 1999) $\Delta\lambda_c = \lambda^2/2L_c$, where L_c is the optical length of the resonator and λ is the laser wavelength. And the center wavelength of the lasers shifts to longer wavelength with the pump power which is caused by the temperature dependent emission spectra of Yb:YAG crystal (Dong et al., 2003). For T_{oc} = 5%, both Yb:YAG ceramic and crystal lasers are oscillating at longer wavelength comparing to those for T_{oc} = 10%. The cause of the wavelength shift to longer wavelength for T_{oc} = 5% is relating to the change of the intracavity laser intensity (Kong et al., 2004) because only the intracavity laser intensity is different for both cases. Intracavity laser intensity for T_{oc} = 5% is about two times higher than that for T_{oc} = 10%, therefore, more longitudinal modes will also be excited for T_{oc} = 5%. Because the better laser performance for 10 at.% Yb:YAG lasers compared to 9.8 at.% Yb:YAG ceramics lasers, the intracavity intensity is higher for crystal laser, therefore Yb:YAG crystal lasers oscillate at longer wavelength than those for Yb:YAG ceramics lasers, especially for T_{oc} = 5%. Strong mode competition and mode hopping in these Yb:YAG ceramic lasers were also observed. When the laser oscillates, the excited Yb^{3+}

ions jump back to the lower laser level, they always relax to other even-lower energy levels or ground level, this process is rapid compare to the lifetime of Yb^{3+} ion in YAG crystal or ceramics. The relaxation of Yb^{3+} ions to the lower energy or ground levels causes the lower-level population to increase with the lasing intensity, this increases the reabsorption. This enhanced reabsorption provides a negative feedback process for the lasing modes and effective gain profile of Yb:YAG medium. This negative feedback process accompanied with the effects of strong mode competition makes some stronger laser modes eventually faded or quenched. When the intracavity light intensity is high enough, the population distribution at lower energy levels is changed dramatically. At the same time, the effective gain curve of Yb:YAG under lasing condition was altered by the strong reabsorption and temperature rise induced by the absorption pump power. Some initially suppressed modes at longer wavelength governed by the emission spectra can oscillate under changed gain curve, therefore the laser wavelength shifts to longer wavelength and mode hopping was observed. Fig. 8 shows the laser emitting spectra of 20 at% Yb:YAG ceramic and single-crystal miniature lasers under different pump power levels and output couplings. The lasers oscillate at multi-longitudinal modes. The number of the longitudinal modes increases with the pump power. The laser oscillates at longer wavelength for 20 at.% Yb:YAG lasers compared to that for 10 at.% Yb:YAG lasers for both transmissions of the output couplers (as shown in Fig. 7 and Fig. 8). The red-shift of laser wavelength for T_{oc} = 10% with Yb concentration is smaller than that for T_{oc} = 5% because of the lower intracavity laser intensity Yb:YAG lasers with T_{oc} = 10%. The number of longitudinal modes is larger for T_{oc} = 5% than that for T_{oc} = 10%. This may be related to the gain curve change due to the strong reabsorption under strong intracavity intensity.

The output beam transverse intensity profiles were also monitored in all the pump power range. One example of the beam intensity profile at output power of 2.5 W for 12 at.%

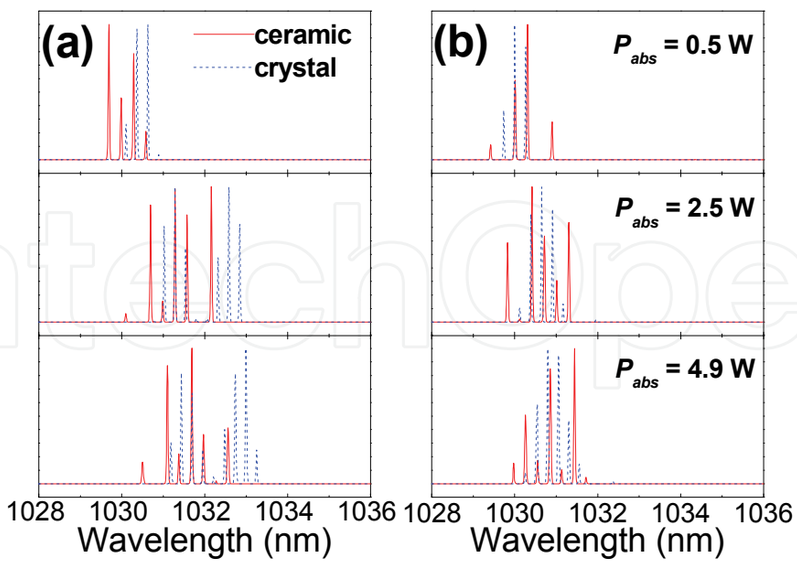

Fig. 7. Laser emitting spectra of 9.8 at.% Yb:YAG ceramic and 10 at.% Yb:YAG crystal miniature lasers under different pump power levels, (a) T_{oc} = 5%, (b) T_{oc} = 10%. The resolution of the optical spectral analyzer is 0.01 nm.

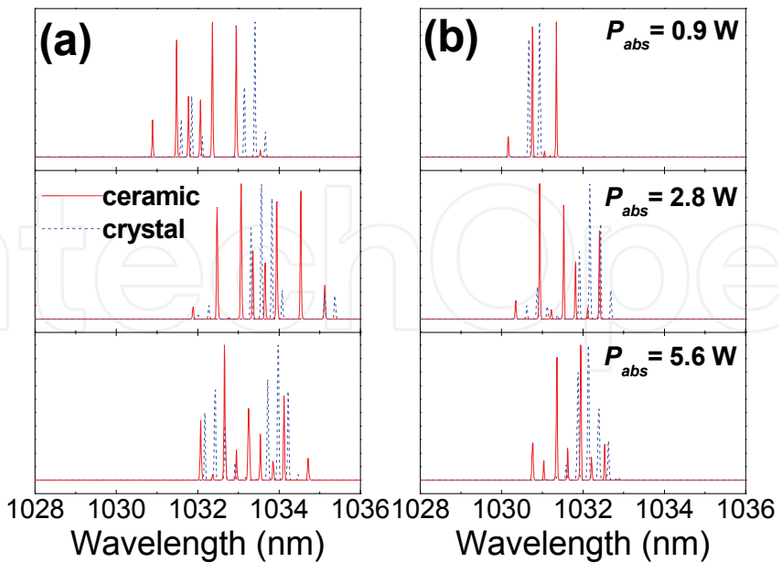

Fig. 8. Laser emitting spectra of 20 at.% Yb:YAG ceramic and crystal miniature lasers under different pump power levels, (a) T_{oc} = 5%, (b) T_{oc} = 10%. The resolution of the optical spectral analyzer is 0.01 nm.

Yb:YAG ceramics with T_{oc} = 5% was shown in Fig. 9, as well as a horizontal slice through the center. The output beam profile is close to TEM_{00} mode. The measured spatial profile can be fitted with Gaussian function very well, as shown in Fig. 9(b). Near-diffraction-limited beam quality with M^2 of less than 1.1 was achieved in these miniature lasers with Yb:YAG ceramics and single-crystals as gain media in the available pump power range.

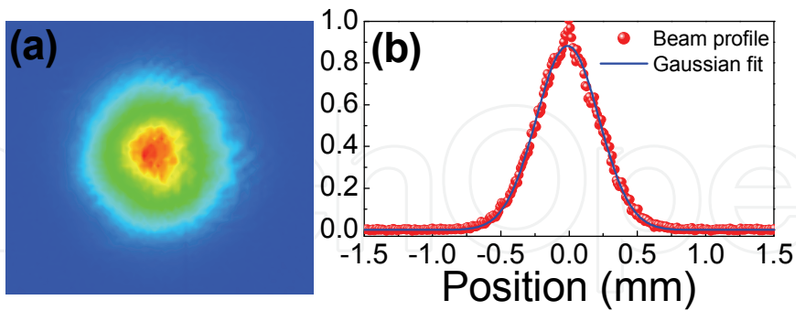

Fig. 9. (a) Output laser beam profile of Yb:YAG ceramic miniature lasers when output power is 2.5 W for 12 at.% Yb:YAG ceramics with T_{oc} = 5%. (b) Horizontal slice through center of beam profile with Gaussian fit.

3.2 Passively Q-switched Yb:YAG/Cr,Ca:YAG microchip lasers

Four combinations of Yb:YAG and Cr,Ca:YAG were used in the laser experiments to investigate the polarization states of passively Q-switched Yb:YAG/Cr,Ca:YAG microchip

lasers: C1, Yb:YAG crystal + Cr,Ca:YAG crystal; C2, Yb:YAG ceramic + Cr,Ca:YAG ceramic; C3, Yb:YAG crystal + Cr,Ca:YAG ceramic; C4, Yb:YAG ceramic + Cr,Ca:YAG crystal. The polarization states of passively Q-switched Yb:YAG/Cr,Ca:YAG microchip lasers with different combinations were investigated by measuring the output power after polarizer. Table 1 summaries the polarization states observed in passively Q-switched Yb:YAG/Cr,Ca:YAG microchip lasers with different combinations of Yb:YAG, Cr,Ca:YAG crystals and ceramics. By rotating the combination of Yb:YAG/Cr,Ca:YAG, the polarization states of these lasers do not change, only the polarization directions are changed by arranging Yb:YAG or Cr,Ca:YAG. Rotating any one of sample does not affect the polarization states and no stronger influence on the polarization was observed.

No.	Combinations	Polarization
C1	Yb:YAG crystal + Cr,Ca:YAG crtstal	Linear
C2	Yb:YAG ceramic + Cr,Ca:YAG ceramic	Random
C3	Yb:YAG crystal + Cr,Ca:YAG ceramic	Linear
C4	Yb:YAG ceramic + Cr,Ca:YAG crystal	Linear

Table 1. Polarizations states of passively Q-switched Yb:YAG/Cr,Ca:YAG microchip lasers

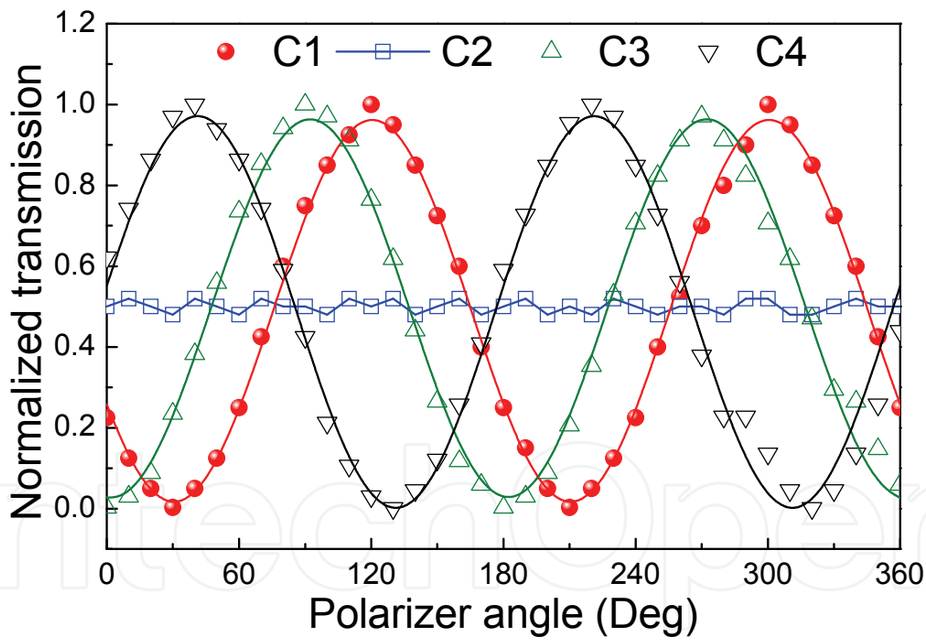

Fig. 10. Polarization states of passively Q-switched Yb:YAG/Cr,Ca:YAG microchip lasers. The solid lines show the sine function fitting of the experimental data.

Fig. 10 shows the typical polarization states of four combinations. Except for the random oscillation of Yb:YAG/Cr,Ca:YAG all-ceramics combination, other three combinations exhibit linearly polarization output. The extinction ratio of the linearly polarization is greater than 300:1. Some differences between the extinction ratios for different linearly polarization were observed. The extinction ratios of three different linearly polarized

combinations are in the order of C1 > C4 > C3. The extinction ratios of three different linearly polarized combinations decrease a little with increase of the pump power, we did not observe significant decrease of the extinction ratio at the maximum pump power used here, this shows that the thermal effect under current available pump power is not strong enough to induce sufficient birefringence and depolarization for Yb:YAG crystals and ceramics. However, we did observe the thermal effect under high pump power level for cw Yb:YAG microchip lasers(Dong et al., 2008), therefore, the thermal effect induced birefringence and depolarization should be considered in high power pumped passively Q-switched Yb:YAG/Cr,Ca:YAG microchip lasers. The different polarization states between all-ceramics combination and three others are due to the random distribution of nanocrystalline particles in ceramics. To fully understand the nature of polarization states in passively Q-switched Yb:YAG/Cr,Ca:YAG microchip lasers, we measured the polarization states of Yb:YAG crystals and ceramics by removing Cr,Ca:YAG saturable absorber and found that Yb:YAG crystals oscillate at linearly polarization states selected by the crystalline-orientations in the (111) plane(Dong et al., 2008) and Yb:YAG ceramic oscillates at unpolarization states. Although there is saturation absorption in Cr,Ca:YAG ceramic, the same as that for Cr,Ca:YAG crystal, owing to the random distribution of Cr,Ca:YAG particles in ceramic, the saturation absorption does not exhibit crystalline-orientation dependent anisotropic properties when the sample is rotated, which is different from the anisotropic saturation absorption of Cr,Ca:YAG crystal when the laser propagate along [111] direction(Eilers et al., 1992). Therefore, the polarization states in passively Q-switched microchip lasers with Cr,Ca:YAG as saturable absorber are not only determined by the anisotropic saturation absorption of Cr,Ca:YAG saturable absorber, but also determined by the linearly polarized states of Yb:YAG crystals.

The continuous-wave operation of Yb:YAG crystal and ceramic has been investigated previously by using different transmissions of output coupler(Dong et al., 2006; Dong et al., 2007) and found that the laser performance 1-mm-thick Yb:YAG crystal doped with 10 at.% Yb is better than that of 1-mm-thick Yb:YAG ceramic doped with 9.8 at.% Yb. The absorbed pump power thresholds are 0.46 W and 0.54 W for 1-mm-thick Yb:YAG crystal and ceramic, respectively, the slope efficiencies were 49% and 44%, respectively by using 50% transmission of output coupler. The differences of cw laser performance between Yb:YAG crystal and ceramic suggest that the optical quality of ceramic used in the experiments is not as good as that of Yb:YAG crystal, and the slight different doping concentration may be another cause of the difference.

Here we show the effect of different polarization states of passively Q-switched Yb:YAG/Cr,Ca:YAG microchip lasers on the laser performance. Average output power as a function of absorbed pump power for these four combinations of Yb:YAG and Cr,Ca:YAG microchip lasers was shown in Fig. 11. The absorbed pump power thresholds were about 0.53, 0.66, 0.75, and 0.6 W for combinations C1, C2, C3 and C4. The higher pump power threshold of these passively Q-switched lasers was due to the low initial transmission of Cr,Ca:YAG and high transmission of the output coupler used in the experiments. Average output power increases linearly with absorbed pump power for the four combinations, the slope efficiencies with respect to the absorbed pump power were estimated to be about 39, 36, 36 and 29% for the four combinations of C1, C2, C3 and C4, respectively. The best laser performance (low threshold and high slope efficiency) of passively Q-switched Yb:YAG/Cr,Ca:YAG microchip lasers was obtained with C1 combination because of the enhancement of linearly polarized laser operation due to the combination of linearly

oscillation of Cr:YAG crystal under high intracavity laser intensity(Eilers et al., 1992) and the crystalline-orientation selected linearly polarized states of Yb:YAG crystal(Dong et al., 2008). Maximum average output power of 310 mw was obtained with Yb:YAG/Cr,Ca:YAG all-crystal combination when the absorbed pump power was 1.34 W, corresponding to optical-to-optical efficiency of 23%. The optical-to-optical efficiency is 15% with respect to the incident pump power for C1. The optical-to-optical efficiencies with respect to the incident pump power were measured to be 12, 11 and 11% for C2, C3 and C4 respectively. There is no coating damage occurrence with further increase of the pump power owing to decrease of the intracavity energy fluence by using high transmission output coupler.

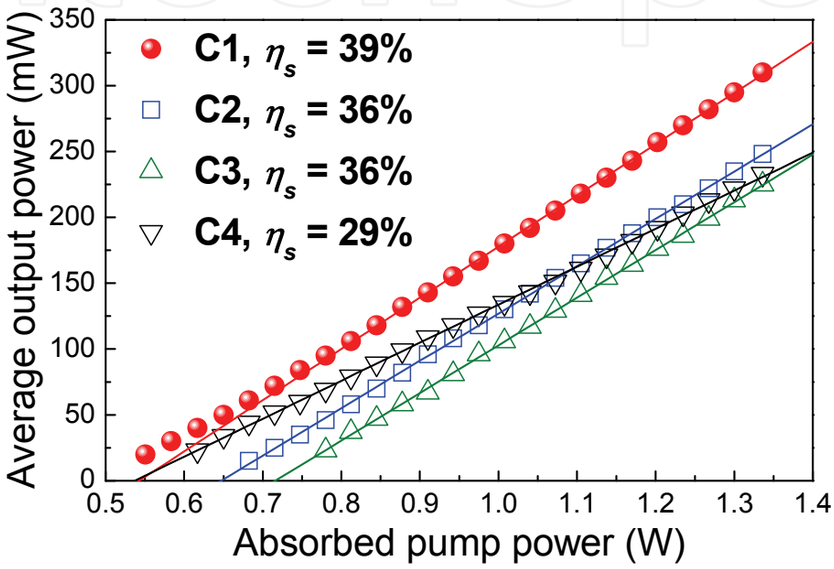

Fig. 11. Average output power as a function of the absorbed pump power for passively Q-switched Yb:YAG/Cr,Ca:YAG microchip lasers with different combinations of Yb:YAG and Cr,Ca:YAG. The solid lines show the linear fit of the experimental data.

Although linearly polarized laser operation was observed in Yb:YAG/Cr,Ca:YAG combinations with at least one crystal, the effect of linearly polarized states on the laser performance was different. The slope efficiency of C4 is lower than that of C3, however the laser threshold of C4 is lower than that of C3 and the average output power is higher than that of C3 for all the available pump power range, as shown in Fig. 11. The contribution of polarization states from Cr,Ca:YAG crystal and Cr,Ca:YAG ceramic is different, when Cr,Ca:YAG crystal is used as saturable absorber, even with Yb:YAG ceramic as gain medium, the laser threshold is low. For all-ceramics combination, C2, although the laser threshold is higher than those of C1 and C4, the slope efficiency is better those of C4 and C3. These results show that the polarized states have great effect on the laser performance. Even with random polarized states of all-ceramics combination, passively Q-switched Yb:YAG/Cr,Ca:YAG laser has nearly the same laser performance as that of all-crystals combination. The discrepancies between all-crystals (C1) and all-ceramics (C2) combinations were caused by the optical quality of Yb:YAG crystal and Yb:YAG ceramic, the laser performance of Yb:YAG crystal is better than its ceramic counterpart. The discrepancies

between C3 and C4 were attributed to the linearly polarization, with Cr,Ca:YAG crystal as saturable absorber, the extinction ratio of the polarization is stronger than that of with Cr,Ca:YAG ceramic as saturable absorber, the laser prefers to oscillate more efficiently with orientation selected anisotropic saturbable absorption of Cr,Ca:YAG crystal along <111> direction under high intracavity intensity(Eilers et al., 1992).

The output beam profile is close to fundamental transverse electro-magnetic mode. Near diffraction-limited output beam quality with M_x^2 of 1.05 and M_y^2 of 1.04, respectively, was achieved in such compact passively-Q-switched Yb:YAG/Cr,Ca:YAG microchip lasers. The output beam diameter near the output mirror was measured to be 100 μm.

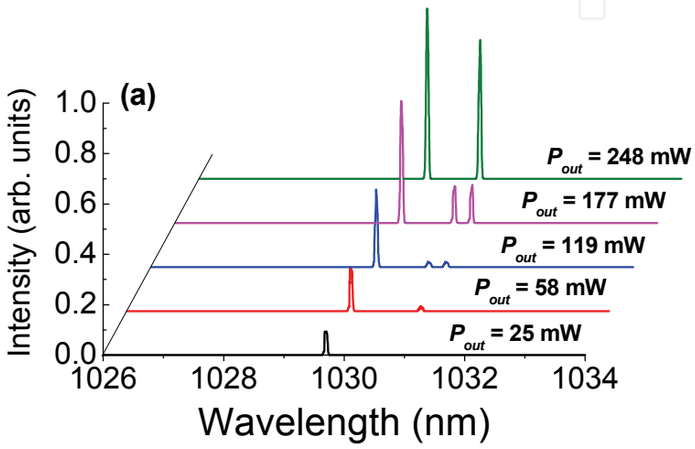

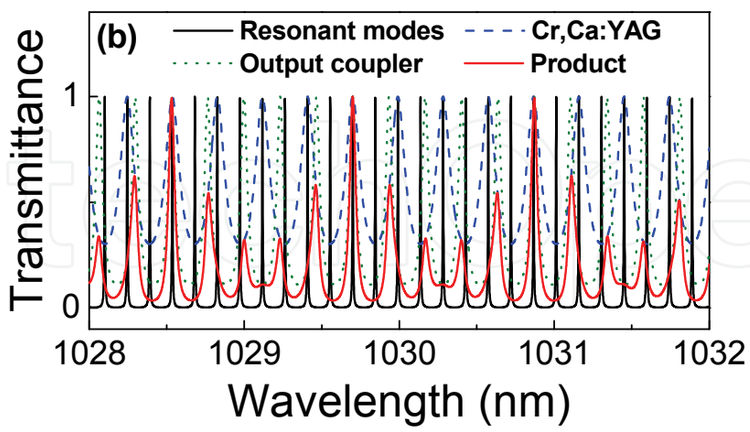

Fig. 12. (a) Laser emission spectra under different average output powers in passively Q-switched Yb:YAG/Cr,Ca:YAG all-ceramic microchip laser; (b) transmittance curves of 1-mm-thick Cr,Ca:YAG, 1.5-mm-thick fused silica output coupler, and their transmittance product. Resonant modes are also plotted for illustration.

Owing to the broad emission spectrum of the Yb:YAG materials around 1.03 μm (about 10 nm in FWHM), many longitudinal modes can be excited even for a 1-mm-thick Yb:YAG crystal. Microchip cw Yb:YAG lasers operate in a multi-longitudinal-mode over the whole pump power region(Dong et al., 2006). However, single-longitudinal-mode oscillation around 1029.7 nm was observed in passively Q-switched Yb:YAG/Cr,Ca:YAG microchip lasers when the average output power was kept below 50 mW for different Yb:YAG/Cr,Ca:YAG combinations, the same as that for all-ceramics combinations(Dong et al., 2007). Above this value, the laser exhibited two-mode oscillation and three-mode oscillation. A typical example of single-longitudinal-mode and multi-longitudinal-mode oscillations of passively Q-switched Yb:YAG/Cr,Ca:YAG all-ceramic microchip laser under different average output power levels is shown in Fig. 12(a). The separation between first and second modes was measured to be 1.16 nm, which is eight times wider than the free spectral range between the longitudinal modes (0.146 nm) in the laser cavity filled with gain medium predicted by(Koechner 1999) $\Delta\lambda_c = \lambda^2/2L_c$, where L_c is the optical length of the resonator and λ is the laser wavelength. The separation between second and third modes was measured to be 0.3 nm, which is twice of that determined by the laser cavity. The potential output longitudinal modes were selected by the combined etalon effect of the 1-mm-thick Cr,Ca:YAG as an intracavity etalon and 1.5-mm-thick fused silica output coupler as a resonant reflector(Koechner 1999). Fig. 12(b) shows the possible selected modes by the combining effect of 1-mm-thick Cr^{4+}:YAG and 1.5-mm-thick fused silica. The resonant modes, eight times of free spectral range (0.146 nm) away from the main mode centered at 1029.7 nm, will oscillate preferably because the wavelengths of these modes are very close to the high transmittance of the combined transmittance product. The resonant mode will oscillate at 1030.87 nm due to the asymmetric gain profile centered at 1029.7 nm of Yb:YAG. At high pump power levels, besides the oscillation of the main mode depleting the inversion population and suppressing the oscillation of the resonant modes close to it, the local temperature rise induced by the pump power will change the transmittance of the etalons. The relative gain and loss for different resonant modes will vary and determine the appearance of the third mode and elimination of the second mode. The linewidth of each mode was less than 0.02 nm, limited by the resolution of optical spectra analyzer. The central wavelength of 1029.7 nm shifts to longer wavelength with pump power, which is caused by the temperature dependent emission spectrum of Yb:YAG crystal(Dong et al., 2003). Therefore, stable single-longitudinal-mode oscillation can be maintained by increasing pump beam diameter incident on the laser medium at higher pump power.

The polarization states of passively Q-switched Yb:YAG/Cr,Ca:YAG microchip lasers have great effect on the characteristics of the output pulses. Fig. 13 shows the pulse characteristics (pulse repetition rate, pulse width, pulse energy and pulse peak power) of passively Q-switched Yb:YAG/Cr,Ca:YAG microchip lasers as a function of absorbed pump power. For all four combinations of Yb:YAG and Cr,Ca:YAG, the repetition rate of passively Q-switched laser increases linearly with the absorbed pump power. Pulse width (FWHM) of passively Q-switched Yb:YAG/Cr,Ca:YAG microchip lasers decreases with absorbed pump power at low pump power levels and tends to keep constant at high pump power levels. The shortest pulse width of 277 ps was achieved with C4 combination. Pulse widths for the four combinations are in the order of C4 < C1 < C2 < C3. Pulse energy increases with absorbed pump power and tends to keep constant at high pump power levels. The highest pulse energy was achieved with C1 combination. The pulse energy for the four

combinations are in the order of C1 > C4 > C2 > C3. Peak power of passively Q-switched Yb:YAG/Cr,Ca:YAG microchip lasers exhibits the same tendency as those of pulse energy: C1 > C4 > C2 > C3 for the four combinations. Therefore, the overall best laser performance (highest peak power) in passively Q-switched Yb:YAG/Cr,Ca:YAG microchip lasers achieved by using C1 combination. Linearly polarization operation of passively Q-switched all-crystals lasers is more favorable for laser performance. The combination of Yb:YAG/Cr,Ca:YAG microchip lasers with Cr,Ca:YAG crystal as saturable absorber, C4, has better laser pulse characteristics than those of all-ceramics combination, C2 and combination C3. Although linearly polarized state was achieved in combination C3 with Yb:YAG crystal, the linearly polarized states was attributed to the linearly polarization of Yb:YAG crystal, not from the Cr,Ca:YAG ceramic. The contribution of the linearly polarized state from Yb:YAG crystal in C3 combination is less than that from the nonlinear anisotropic absorption of Cr,Ca:YAG crystal, therefore, therefore, the laser performance of combination C3 is less than those of combination C1 and C4. The effect of depolarization effect on the polarization states observed in Yb:YAG crystal (Dong et al., 2008) may be another cause to less efficient laser operation in C3 combination at high pump power levels.

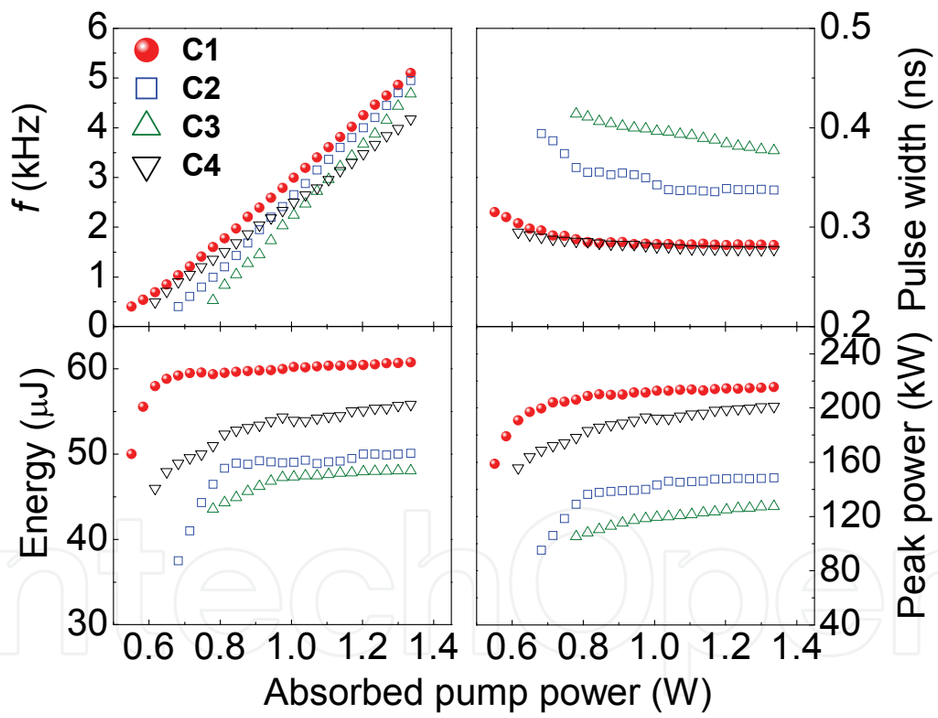

Fig. 13. Pulse characteristics (repetition rate, pulse width, pulse energy and peak power) of passively Q-switched Yb:YAG/Cr,Ca:YAG microchip lasers as a function of absorbed pump power for different combinations of Yb:YAG and Cr,Ca:YAG.

4. Conclusions

In conclusion, systematic comparison of laser performance was done for Yb:YAG ceramics and single-crystals doped with different concentrations. Although the pump power

thresholds of Yb:YAG crystals were higher than their ceramics counterparts due to the pump configuration, the efficient laser operation was obtained by using both Yb;YAG ceramics and single-crystals. The laser performance of 1-mm-thick Yb:YAG ceramics and crystals becomes worse with Yb concentration under present miniature laser configuration. However, the laser performance of Yb:YAG crystals is more sensitive to the Yb concentrations, while the laser performance of Yb:YAG ceramics is less sensitive to the Yb concentrations. The laser performance of low doping Yb:YAG ceramics is worse than those obtaining from Yb:YAG singly crystals. The laser performance of 20 at.% Yb:YAG ceramics is better than its counterpart single crystal. Both Yb:YAG ceramics and crystals miniature lasers oscillate at multi-longitudinal modes, the number of longitudinal-mode increases with absorbed pump power. Strong mode competition and mode hopping were observed in these Yb:YAG lasers. The strong reabsorption and gain curve change under high intracavity laser intensity play important roles on the red-shift of the output laser wavelength. High beam quality lasers with M^2 less than 1.1 were achieved by adopting Yb:YAG ceramics and crystals as gain media. Heavy-doped Yb:YAG ceramic will be a potential candidate for microchip lasers by optimizing the thickness and Yb^{3+} concentration.

Random polarized oscillation was observed in passively Q-switched Yb:YAG/Cr,Ca:YAG all-ceramic microchip laser while linearly polarized oscillations were observed with at lease one crystal in the Yb:YAG/Cr,Ca:YAG combinations. The polarization states in passively Q-switched Yb:YAG/Cr,Ca:YAG microchip lasers show that the linearly polarization states in passively Q-switched laser are not only resulted from the anisotropic saturation absorption of Cr,Ca:YAG crystal, but also from linearly polarization states of Yb:YAG crystal. High peak power pulses with sub-nanosecond pulse-width and nearly diffraction-limited beam quality were obtained in these lasers. The best laser performance was achieved by using Yb:YAG crystal as gain medium and Cr,Ca:YAG crystal as saturable absorber because of the enhancement of linearly polarized state due to the crystalline-orientation selected polarized states of Yb:YAG crystal and linearly polarized oscillation of Cr,Ca:YAG crystal under high intracavity laser intensity. Other combinations of Yb:YAG and Cr,Ca:YAG have less efficient linearly polarized laser oscillation and also affect the laser performance of passively Q-switched Yb:YAG/Cr,Ca:YAG microchip lasers.

5. References

Barabanenkov, Y. N., Ivanov, S. N., Taranov, A. V., Khazanov, E. N., Yagi, H., Yanagitani, T., Takaichi, K., Lu, J., Bisson, J. F., Shirakawa, A., Ueda, K. & Kaminskii, A. A. (2004). Nonequilibrium acoustic phonons in $Y_3Al_5O_{12}$-based nanocrystalline ceramics. *JETP Lett.* Vol. 79, No. 7, (342 - 345).

Bisson, J., Yagi, H., Yanagitani, T., Kaminskii, A., Barabanenkov, Y. N. & Ueda, K. (2007). Influence of the grain boundaries on the heat transfer in laser ceramics. *Opt. Rev.* Vol. 14, No. 1, (1 - 13).

Bogomolova, G. A., Vylegzhanin, D. N. & Kaminskii, A. A. (1976). Spectral and lasing investigations of garnets with Yb^{3+} ions. *Sov. Phys. JETP* Vol. 42, No. 3, (440 - 446).

Bouwmans, G., Segard, B. & Glorieux, P. (2001). Polarisation dynamics of monomode Nd^{3+}:YAG lasers with Cr^{4+} saturable absorber: influence of the pump polarisation. *Opt. Commun.* Vol. 196, No. 1-6, (257 - 268).

Brauch, U., Giesen, A., Karszewski, M., Stewen, C. & Voss, A. (1995). Multiwatt diode-pumped Yb:YAG thin disk laser continuously tunable between 1018 and 1053 nm. *Opt. Lett.* Vol. 20, No. 7, (713 - 715).

Bruesselbach, H. W., Sumida, D. S., Reeder, R. A. & Byren, R. W. (1997). Low-heat high-power scaling using InGaAs-diode-pumped Yb:YAG lasers *IEEE J. Sel. Top. Quantum Electron.* Vol. 3, No. 1, (105 - 116).

Degnan, J. J. (1995). Optimization of passively Q-switched lasers. *IEEE J. Quantum Electron.* Vol. 31, No. 11, (1890 - 1901).

Dobrzycki, L., Bulska, E., Pawlak, D. A., Frukacz, Z. & Wozniak, K. (2004). Structure of YAG crystals doped/substituted with erbium and ytterbium. *Inorg. Chem.* Vol. 43, No. 24, (7656 - 7664).

Dong, J., Bass, M., Mao, Y., Deng, P. & Gan, F. (2003). Dependence of the Yb^{3+} emission cross section and lifetime on the temperature and concentration in ytterbium aluminum garnet. *J. Opt. Soc. Am. B* Vol. 20, No. 9, (1975 - 1979).

Dong, J., Deng, P., Lu, Y., Zhang, Y., Liu, Y., Xu, J. & Chen, W. (2000). LD pumped Cr^{4+},Nd^{3+}:YAG with self-Q-switched laser output of 1.4 W. *Opt. Lett.* Vol. 25, No. 15, (1101 - 1103).

Dong, J., Shirakawa, A., Takaichi, K., Ueda, K., Yagi, H., Yanagitani, T. & Kaminskii, A. A. (2006). All ceramic passively Q-switched Yb:YAG/Cr^{4+}:YAG microchip laser. *Electron. Lett.* Vol. 42, No. 20, (1154 - 1156).

Dong, J., Shirakawa, A. & Ueda, K. (2008). A crystalline-orientation self-selected linearly polarized Yb:$Y_3Al_5O_{12}$ microchip laser. *Appl. Phys. Lett.* Vol. 93, No. 10, (101105).

Dong, J., Shirakawa, A., Ueda, K. & Kaminskii, A. A. (2007). Effect of ytterbium concentration on CW Yb:YAG microchip laser performance at ambient temperature Part I: Experiments. *Appl. Phys. B* Vol. 89, No. 2-3, (359 - 365).

Dong, J., Shirakawa, A., Ueda, K., Xu, J. & Deng, P. (2006). Efficient laser oscillation of Yb:$Y_3Al_5O_{12}$ single crystal grown by temperature gradient technique. *Appl. Phys. Lett.* Vol. 88, No. 16, (161115).

Dong, J., Shirakawa, A., Ueda, K., Yagi, H., Yanagitani, T. & Kaminskii, A. A. (2006). Efficient Yb^{3+}:$Y_3Al_5O_{12}$ ceramic microchip lasers. *Appl. Phys. Lett.* Vol. 89, No. 9, (091114).

Dong, J., Shirakawa, A., Ueda, K., Yagi, H., Yanagitani, T. & Kaminskii, A. A. (2007). Laser-diode pumped heavy doped Yb:YAG ceramic lasers. *Opt. Lett.* Vol. 32, No. 13, (1890 -1892).

Dong, J., Shirakawa, A., Ueda, K., Yagi, H., Yanagitani, T. & Kaminskii, A. A. (2007). Near-diffraction-limited passively Q-switched Yb:$Y_3Al_5O_{12}$ ceramic lasers with peak power > 150 kW. *Appl. Phys. Lett.* Vol. 90, No. 13, (131105).

Dong, J., Shirakawa, A., Ueda, K., Yagi, H., Yanagitani, T. & Kaminskii, A. A. (2007). Ytterbium and chromium doped composite $Y_3Al_5O_{12}$ ceramics self-Q-switched laser. *Appl. Phys. Lett.* Vol. 90, No. 19, (191106).

Dong, J. & Ueda, K. (2005). Temperature-tuning Yb:YAG microchip lasers. *Laser Phys. Lett.* Vol. 2, No. 9, (429 - 436).

Dong, J., Ueda, K., Shirakawa, A., Yagi, H., Yanagitani, T. & Kaminskii, A. A. (2007). Composite Yb:YAG/Cr^{4+}:YAG ceramics picosecond microchip lasers. *Opt. Express* Vol. 15, No. 22, (14516 - 14523).

Eilers, H., Hoffman, K. R., Dennis, W. M., Jacobsen, S. M. & Yen, W. M. (1992). Saturation of 1.064 μm absorption in Cr,Ca:$Y_3Al_5O_{12}$ crystals. *Appl. Phys. Lett.* Vol. 61, No. 25, (2958 -2960).

Fan, T. Y. (1993). Heat generation in Nd:YAG and Yb:YAG. *IEEE J. Quantum Electron.* Vol. 29, No. 6, (1457 -1459).

Fan, T. Y. & Ochoa, J. (1995). Tunable single-frequency Yb:YAG laser with 1-W output power using twisted-mode technique. *IEEE Photon. Technol. Lett.* Vol. 7, No. 10, (1137 -1138).

Feng, Y., Lu, J., Takaichi, K., Ueda, K., Yagi, H., Yanagitani, T. & Kaminskii, A. A. (2004). Passively Q-switched ceramic Nd^{3+}:YAG/Cr^{4+}:YAG lasers. *Appl. Opt.* Vol. 43, No. 14, (2944 - 2947).

Giesen, A., Hugel, H., Voss, A., Wittig, K., Brauch, U. & Opower, H. (1994). Scalable concept for diode-pumped high-power solid-state lasers. *Appl. Phys. B* Vol. 58, No. 5, (365 - 372).

Honea, E. C., Beach, R. J., S. C. Mitchell, Sidmore, J. A., M. A. Emanuel, Sutton, S. B., Payne, S. A., Avizonis, P. V., Monroe, R. S. & Harris, D. (2000). High-power dual-rod Yb:YAG laser. *Opt. Lett.* Vol. 25, No. 11, (805 - 807).

Kir'yanov, A. V., Aboites, V. & Ii'ichev, N. N. (1999). A polarisation-bistable noedymium laser with a Cr^{4+}:YAG passive switch under the weak resonant signal control. *Opt. Commun.* Vol. 169, No. 1-6, (309 - 316).

Koechner, W. (1999). *Solid State Laser Engineering*. Berlin, Springer-Verlag.

Kong, J., Tang, D. Y., Lu, J. & Ueda, K. (2004). Random-wavelength solid-state laser. *Opt. Lett.* Vol. 29, No. 1, (65 - 67).

Krupke, W. F. (2000). Ytterbium solid-state lasers - The first decade. *IEEE J. Sel. Top. Quantum Electron.* Vol. 6, No. 6, (1287 - 1296).

Lacovara, P., Choi, H. K., Wang, C. A., Aggarwal, R. L. & Fan, T. Y. (1991). Room-temperature diode-pumped Yb:YAG laser. *Opt. Lett.* Vol. 16, No. 14, (1089 - 1091).

Lagatsky, A. A., Abdolvand, A. & Kuleshov, N. V. (2000). Passive Q-switching and self-frequency Raman conversion in a diode-pumped Yb:$KGd(WO_4)_2$ laser. *Opt. Lett.* Vol. 25, No. 9, (616 - 618).

Li, S., Zhou, S., Wang, P., Chen, Y. C. & Lee, K. K. (1993). Sefl-Q-switched diode-end-pumped Cr,Nd:YAG laser with polarized output. *Opt. Lett.* Vol. 18, No. 3, (203 - 204).

Lu, J., Prabhu, M., Song, J., Li, C., Xu, J., Ueda, K., Kaminskii, A. A., Yagi, H. & Yanagitani, T. (2000). Optical properties and highly efficient laser oscillation of Nd:YAG ceramics. *Appl. Phys. B* Vol. 71, No. 4, (469 - 473).

Lu, J., Prabhu, M., Song, J., Li, C., Xu, J., Ueda, K., Yagi, H., Yanagitani, T. & Kaminskii, A. A. (2001). Highly efficient Nd:$Y_3Al_5O_{12}$ ceramic laser. *Jpn. J. Appl. Phys.* Vol. 40, No. 6A, (L552 - L554).

Lu, J., Ueda, K., Yagi, H., Yanagitani, T., Akiyama, Y. & Kaminskii, A. A. (2002). Neodymium-doped yttrium aluminum garnet ($Y_3Al_5O_{12}$) nanocrystalline ceramics - a new generation of solid-state laser and optical materials. *J. Alloys Compd.* Vol. 341, No. 1-2, (220 - 225).

M. Ito, C. Goutaudier, Y. Guyot, K. Lebbou, T. Fukuda & Boulon, G. (2004). Crystal growth, Yb^{3+} spectroscopy, concentration quenching analysis and potentiality of laser emission in $Ca_{1-x}Yb_xF_{2+x}$. *J. Phys.: Condens. Matter* Vol. 16, No. 8, (1501 - 1521).

McKay, A., Dawes, J. M. & Park, J. (2007). Polarisation-mode coupling in (100)-cut Nd:YAG. *Opt. Express* Vol. 15, No. 25, (16342 - 16347).

Nakamura, S., Yoshioka, H., Matsubara, Y., Ogawa, T. & Wada, S. (2008). Efficient tunable Yb:YAG ceramic laser. *Opt. Commun.* Vol. 281, No. 17, (4411 - 4414).

Okhrimchuk, A. G. & Shestakov, A. V. (1994). Performance of YAG: Cr^{4+} laser crystal. *Opt. Mater.* Vol. 3, No. 1, (1 - 13).

Patel, F. D., Honea, E. C., Speth, J., Payne, S. A., Hutcheson, R. & Equall, R. (2001). Laser demonstration of $Yb_3Al_5O_{12}$ (YAG) and materials properties of highly doped Yb:YAG. *IEEE J. Quantum Electron.* Vol. 37, No. 1, (135 - 144).

Qiu, H., Yang, P., Dong, J., Deng, P., Xu, J. & Chen, W. (2002). The influence of Yb concentration on laser crystal Yb:YAG. *Mater. Lett.* Vol. 55, No. 1-2, (1 - 7).

Rutherford, T. S., Tulloch, W. M., Gustafson, E. K. & Byer, R. L. (2000). Edge-pumped quasi-three-level slab lasers: design and power scaling. *IEEE J. Quantum Electron.* Vol. 36, No. 2, (205 - 219).

Spuhler, G. J., Paschotta, R., Kullberg, M. P., Graf, M., Moser, M., Mix, E., Huber, G., Harder, C. & Keller, U. (2001). A passively Q-switched Yb:YAG microchip laser. *Appl. Phys. B: Lasers Opt.* Vol. 72, No. 3, (285 - 287).

Stewen, C., Contag, K., Larionov, M., Giessen, A. & Hugel, H. (2000). A 1-kW CW Thin Disc laser. *IEEE J. Sel. Top. Quantum Electron.* Vol. 6, No. 4, (650 -657).

Sumida, D. S. & Fan, T. Y. (1994). Effect of radiation trapping on fluorescence lifetime and emission cross section measurements in solid-state laser media *Opt. Lett.* Vol. 19, No. 17, (1343 - 1345).

Taira, T., Saikawa, J., Kobayashi, T. & Byer, R. L. (1997). Diode-pumped tunable Yb:YAG miniature lasers at room temperature: modeling and experiment. *IEEE J. Sel. Top. Quantum Electron.* Vol. 3, No. 1, (100 - 104).

Takaichi, K., Lu, J., Murai, T., Uematsu, T., Shirakawa, A., Ueda, K., Yagi, H., Yanagitani, T. & Kaminskii, A. A. (2002). Chromium-doped $Y_3Al_5O_{12}$ ceramics - a novel saturable absorber for passively self-Q-switched 1-μm solid-state lasers. *Jpn. J. Appl. Phys.* Vol. 41, No. 2A, (L96 - L98).

Takaichi, T., Yagi, H., Lu, J., Shirakawa, A., Ueda, K., Yanagitani, T. & Kaminskii, A. A. (2003). Yb^{3+}-doped $Y_3Al_5O_{12}$ ceramics - A new solid-state laser material. *Phys. Status Solidi (a)* Vol. 200, No. 1, (R5 - R7).

Xu, X., Zhao, Z., Song, P., Jiang, B., Zhou, G., Xu, J., Deng, P., Bourdet, G., Chanteloup, J. C., Zou, J. & Fulop, A. (2005). Upconversion luminescence in Yb^{3+} - doped yttrium aluminum garnets. *Physica B* Vol. 357, No. 3 -4, (365 - 369).

Xu, X., Zhao, Z., Zhao, G., Song, P., Xu, J. & Deng, P. (2003). Comparison of Yb:YAG crystals grown by CZ and TGT method. *J. Crystal Growth* Vol. 257, No. 3-4, (297 - 300).

Yagi, H., Yanagitani, T., Yoshida, K., Nakatsuka, M. & Ueda, K. (2006). Highly efficient flashlamp-pumped Cr^{3+} and Nd^{3+} codoped $Y_3Al_5O_{12}$ ceramic laser. *Jpn. J. Appl. Phys.* Vol. 45, No. 1A, (133 - 135).

Yanagitani, T., Yagi, H. & Hiro, Y. (1998). Production of yttrium aluminium garnet fine powders for transparent YAG ceramic. Japan Patent 10-101411.

Yang, P., Deng, P. & Yin, Z. (2002). Concentration quenching in Yb:YAG. *J. Lumin.* Vol. 97, No. 1, (51 - 54).

Yankov, P. (1994). Cr^{4+}:YAG Q-switching of Nd:host laser oscillators. *J. Phys. D* Vol. 27, No. 6, (1118 - 1120).

Yin, H., Deng, P. & Gan, F. (1998). Defects in YAG:Yb crystal. *J. Appl. Phys.* Vol. 83, No. 7, (3825 - 3828).

Yoshino, T. & Kobyashi, Y. (1999). Temperature characteristics and stabilization of orthogonal polarization two-frequency Nd^{3+}:YAG microchip lasers. *Appl. Opt.* Vol. 38, No. 15, (3266 - 3270).

Zayhowski, J. J. (2000). Passively Q-switched Nd:YAG microchip lasers and applications. *J. Alloys Comp.* Vol. 303-304, No. (393 - 400).

Zayhowski, J. J. & Dill III, C. (1994). Diode-pumped passively Q-switched picosecond microchip lasers. *Opt. Lett.* Vol. 19, No. 18, (1427 -1429).

Advances in Solid State Lasers Development and Applications

Edited by Mikhail Grishin

ISBN 978-953-7619-80-0
Hard cover, 630 pages
Publisher InTech
Published online 01, February, 2010
Published in print edition February, 2010

Invention of the solid-state laser has initiated the beginning of the laser era. Performance of solid-state lasers improved amazingly during five decades. Nowadays, solid-state lasers remain one of the most rapidly developing branches of laser science and become an increasingly important tool for modern technology. This book represents a selection of chapters exhibiting various investigation directions in the field of solid-state lasers and the cutting edge of related applications. The materials are contributed by leading researchers and each chapter represents a comprehensive study reflecting advances in modern laser physics. Considered topics are intended to meet the needs of both specialists in laser system design and those who use laser techniques in fundamental science and applied research. This book is the result of efforts of experts from different countries. I would like to acknowledge the authors for their contribution to the book. I also wish to acknowledge Vedran Kordic for indispensable technical assistance in the book preparation and publishing.

InTech Europe
University Campus STeP Ri
Slavka Krautzeka 83/A
51000 Rijeka, Croatia
Phone: +385 (51) 770 447
Fax: +385 (51) 686 166
www.intechopen.com

InTech China
Unit 405, Office Block, Hotel Equatorial Shanghai
No.65, Yan An Road (West), Shanghai, 200040, China
中国上海市延安西路65号上海国际贵都大饭店办公楼405单元
Phone: +86-21-62489820
Fax: +86-21-62489821

IntechOpen